

Whispering-gallery mode microdisk lasers

S. L. McCall, A. F. J. Levi, R. E. Slusher, S. J. Pearton, and R. A. Logan
AT&T Bell Laboratories, 600 Mountain Avenue, Murray Hill, New Jersey 07974

(Received 10 September 1991; accepted for publication 18 November 1991)

A new microlaser design based on the high-reflectivity whispering-gallery modes around the edge of a thin semiconductor microdisk is described and initial experimental results are presented. Optical confinement within the thin disk plane results in a microresonator with potential for single-mode, ultralow threshold lasers. Initial experiments use selective etching techniques in the InP/InGaAsP system to achieve 3–10 μm diameter disks as thin as 500 Å suspended in air or SiO₂ on an InP pedestal. Optically pumped InGaAs quantum wells provide sufficient gain when cooled with liquid nitrogen to obtain single-mode lasing at 1.3 and 1.5 μm wavelengths with threshold pump powers below 100 μW .

New ideas are needed if optical or optoelectronic devices will ever succeed in replacing any of the functionality of a purely electronic large-scale integrated circuit. A first requirement for a photonic or optoelectronic circuit is low-power consumption for the constituent devices. In addition, light must be generated and spatially confined to micron size dimensions to ensure both integrability and the possibility of complex functionality on a single chip. In order to meet these challenging demands, novel optical microstructures that strongly confine the optical fields must be designed and fabricated. In this letter we propose and demonstrate lasing action in a new class of microstructures based on the large dielectric discontinuity between an optically thin semiconductor layer and a surrounding low index medium. These microlasers have potential for the integrability and low-power operation required for large-scale photonic circuits.

Our microcavity design incorporates both high reflectivity and matching between a small gain volume and a single optical mode required for ultralow laser thresholds. Optical modes at the edge of a thin semiconductor dielectric disk, similar to whispering-gallery modes,^{1–4} are used because of their high reflectivities. Optical gain for the disk modes is provided by one or more optically pumped quantum wells in the plane of the disk. The disk thicknesses are less than $\lambda/2n_D \approx 2000$ Å, for a wavelength $\lambda = 1.5$ μm and a disk index of refraction $n_D = 3.5$. A low index medium surrounds each disk, either air ($n = 1$) or SiO₂ ($n = 1.5$). This high index contrast ratio between the disk and its surroundings is a key feature of the design in that it strongly confines the active optical modes to the plane of the disk so that a major fraction of the mode overlaps with the quantum well gain layer. The high index contrast ratio also enhances the high reflectivity and mode selectivity of the microcavity.

The modes of a thin dielectric disk are complicated solutions of Maxwell's equations, but many relevant properties may be found through general arguments. For example, dielectric sheets less than $\lambda/2n_D$ thick support only the lowest order TE and TM guided waves.⁵ If the thickness is $\sim \lambda/4n_D$, coupling to the TE mode dominates to the point where interactions with the TM modes and all unguided waves can be neglected, i.e., their effective coupling to the gain medium is less than 10% that of the TE mode.⁵

The requirement that the field wave vector components parallel to the dielectric sheet edge must be equal across the sheet edge results in total internal reflection at a sheet edge for incident angles larger than $\sin^{-1}(1/n_{\text{eff}})$, where n_{eff} is the velocity of light divided by the phase velocity in the thin dielectric sheet. A thin dielectric disk will therefore support modes similar to whispering-gallery modes, where photons skim along the circumference being continually totally reflected. Two mode numbers may be introduced for the field in the disk: M corresponding to the azimuthal angle ϕ in cylindrical coordinates, and a radial number N , where $N - 1$ denotes the number of nodes along the radius r . Cylindrical symmetry implies that the field mode functions are characterized by a factor $\exp(iM\phi)$ with mode degeneracy two (M and $-M$). Any defect around the circumference of the disk will remove this degeneracy. The factor of $\exp(iM\phi)$ in the wave equation solution is associated with a repulsive angular momentum potential that varies as M^2/r^2 . This repulsive potential in combination with the attractive potential within the dielectric disk combine to form a potential trough just inside the disk edge and a tunneling barrier outside the disk extending to a radius $r \approx M\lambda/2\pi \approx n_{\text{eff}}R_D$, where R_D is the disk radius. Thus waves propagating outward from the disk into the surrounding low index region are evanescent while tunneling out to a radius $r = n_{\text{eff}}R_D$ and then propagate freely outward from the disk. An intensity profile of a whispering-gallery mode, the evanescent region and the free-propagation region are shown in Fig. 1. Using the WKB approximation to estimate tunneling rates, we find a cavity Q

$$Q \approx \exp(2MJ), \quad (1)$$

where

$$J = \tanh[(1 - 1/n_{\text{eff}}^2)^{1/2}] - (1 - 1/n_{\text{eff}}^2)^{1/2}. \quad (2)$$

Comparison of this estimate with Q values calculated for whispering-gallery modes of a dielectric sphere indicates that Eq. (1) over estimates Q by a factor of ~ 6.5 for the $M = 8$ mode. Large Q values are predicted for relatively small M , e.g., $Q = 186$ is estimated for the $M = 8$, $n_{\text{eff}} = 2$ mode from Eq. (1) with the correction factor of 6.5. However, at large M the mode spectral density increases to a point where an undesirably large number of

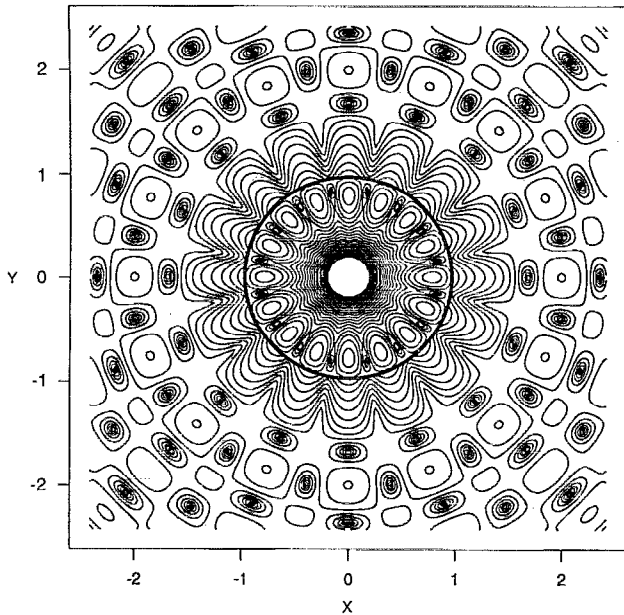


FIG. 1. Approximate calculation of the intensity pattern for a $M=8$, $N=1$ whispering-gallery mode is shown corresponding to the plane of a $2\text{-}\mu\text{m}$ -diam disk with a thickness such that $n_{\text{eff}}=2$. Contour lines are shown at 3 dB intervals. The disk edge is shown as a circle. There are $2M=16$ intensity nodes around the disk. Note the exponentially decaying intensity in the tunneling barrier region $R_D < r < n_{\text{eff}}R_D$. Beyond this region the waves begin to propagate freely. This intensity map is calculated for a dielectric sphere which should approximate the disk intensity patterns.

modes occupy the gain spectrum. Of course, this mode density decreases with disk radius, so that $R_D \approx 1\ \mu\text{m}$ with $M \approx 8$ (Fig. 1) appears to be an optimum choice of parameters.

A perfect disk mode emits radiation into a relatively narrow range of angles about the disk plane compared with the diffraction angle associated with the disk thickness. This angular narrowing of the whispering-gallery mode emission is the result of the tunneling barrier described above. The full width half maximum edge-emission angle is estimated to be $2/\sqrt{M}$ ($\approx 23^\circ$ for a $5\text{-}\mu\text{m}$ -diam disk). The disk must be isolated from any high index supporting structure by a distance large enough to avoid strong coupling of the whispering-gallery mode into the substrate. This typically requires high index support structures to be removed by several wavelengths from the edge of the disk.

Microdisks for our experiments were fabricated on organometallic vapor phase epitaxially grown InP/InGaAsP layered material. A series of InGaAs quantum wells $100\ \text{\AA}$ thick separated by $100\ \text{\AA}$ InGaAsP barriers with $200\ \text{\AA}$ InGaAsP end caps is initially grown on an InP substrate. The total thickness of this well/barrier region was $500\ \text{\AA}$ for a single-well disk and $1500\ \text{\AA}$ for a six-well disk. The band-gap wavelength for the barrier material is $1.3\ \mu\text{m}$ for the single-well and $1.1\ \mu\text{m}$ for the six-well disks. Photolithographic techniques were used to pattern cylinders with diameters of 3, 5, and $10\ \mu\text{m}$. A HCl solution was used to selectively etch away the InP around and below the quantum wells while leaving a InGaAsP well/barrier disk un-

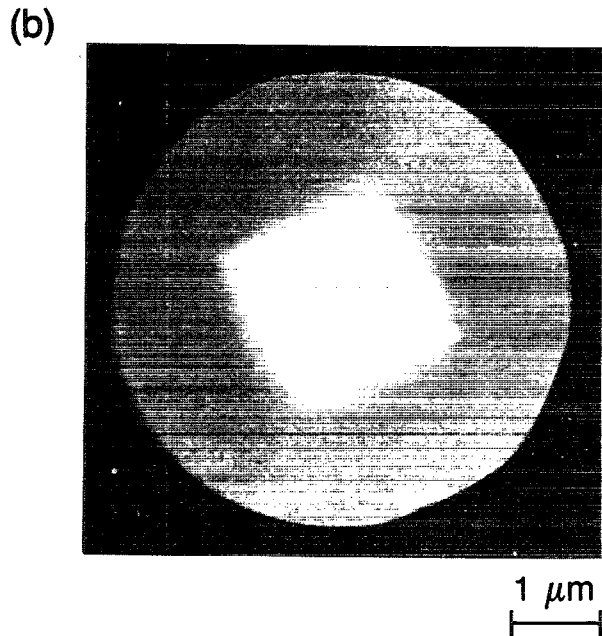
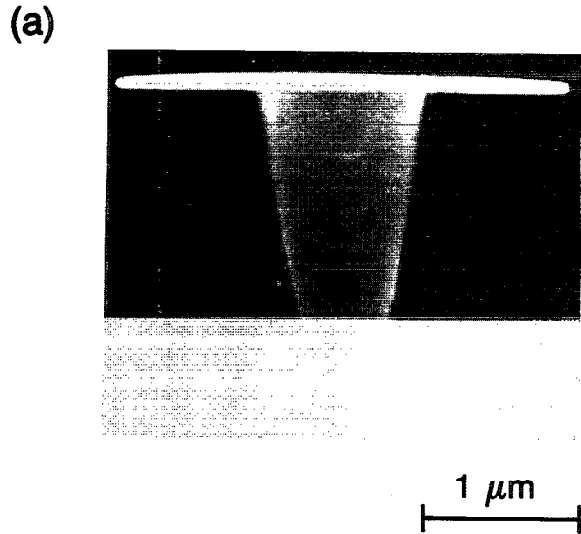


FIG. 2. Scanning electron microscope images of the microdisks are shown in (a) a side view and (b) a top view. In (a) the disk diameter is $3\ \mu\text{m}$ and in (b) the diameter is $5\ \mu\text{m}$. The InP pedestal is a rhombus in cross section as seen in the top view. It tapers to smaller dimensions as it approaches the substrate. The background contrast has been enhanced in this figure to improve its visibility in the journal format.

etched. Scanning electron microscope images of the resulting disk structures are shown in Fig. 2. The side view of a $3\text{-}\mu\text{m}$ -diam disk shows a $500\text{-}\text{\AA}$ -thick disk consisting of one $100\ \text{\AA}$ InGaAs well between two $200\ \text{\AA}$ InGaAsP barriers suspended in air on an InP pedestal $\sim 1\ \mu\text{m}$ on a side and $2\ \mu\text{m}$ in height. A top view of a $5\text{-}\mu\text{m}$ -diam disk shows that the pedestal is a rhombus in cross section due to the anisotropic HCl etch. Surprisingly, these beautiful microcavities are very robust.

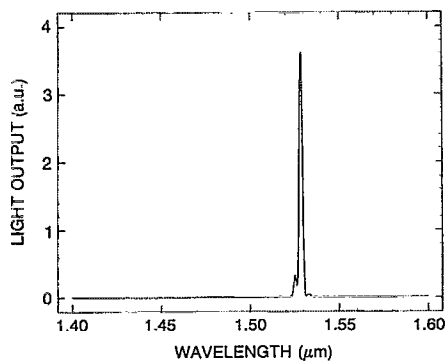


FIG. 3. Spectrum of a lasing line is shown for a 5- μm -diam disk with six 100 \AA InGaAs quantum wells. The apparent spectral structure of the laser line is due to the spectrometer.

The microdisks shown in Fig. 2 deviate from an ideal disk in two important aspects. First, the InP pedestal results in optical losses for disk modes that significantly overlap the pedestal. This limits the number of low-loss modes near the edge and also provides for coupling radiation into the vertical direction, perpendicular to the plane of the disk. Second, roughness at the disk edge introduces scattering losses that may decrease the effective cavity Q and increase the thresholds for lasing.

Microdisks similar to those shown in Fig. 2(b) with six quantum wells exhibited lasing spectra as shown in Fig. 3 when optically pumped with a 0.63 μm HeNe laser. The laser line intensity is over a factor of a hundred larger than the peak of the background photoluminescence. These structures lased with substrate temperatures as high as 0 $^{\circ}\text{C}$. Output from the microdisk was measured from above with a microscope objective collecting only 7% of 4π steradians. The measured microdisk laser power into the collection cone is approximately 1 μW for a pump power near 500 μW . The total microdisk laser power output has not been measured since it includes the emission into a wide range of solid angles and into the substrate. We think that the emission pattern and the actual Q of the cavity are probably dominated by scattering from imperfections in the present structures. The spectral linewidth of the lasing line is less than the 1 \AA resolution of the spectrometer. Threshold pump powers were in the 50 to 100 μW range for the six quantum well microdisks in rough agreement with an estimate of the pump power required to obtain transparency of the quantum wells throughout the disk. The single quantum well disks had higher thresholds near 200 μW and lased at wavelengths near 1.3 μm , probably due to a combination of band-filling and gain enhancement from the 1.3 μm barriers used for these microdisks. If the pump can be confined to only the whispering-gallery mode at the edge of a 2 μm diam. disk, threshold powers less than 2 μW are predicted. Heat sinking sufficient to prevent excessive temperature rises can be obtained through the supporting pedestal as long as the cw pump powers are well below 1 mW. The 3 μm diam. microdisks did not lase because the small dimensions of their pedestals in the

present experiments did not provide sufficient heat sinking for cw pumping.

As the pump power was decreased the lasing mode often switched to a neighboring mode shifted 0.06 μm to shorter wavelengths in the 5- μm -diam, 1500- \AA -thick disks. This mode spacing is consistent with a whispering-gallery mode jump from M to $M + 1$ with $M \approx \lambda/0.06 \approx 25$. This is in good agreement with the estimate of $M = 2\pi R_D n_{\text{eff}}/\lambda \approx 26$ with $n_{\text{eff}} \approx 2.5$ as calculated for a 1500- \AA -thick, $n = 3.5$ dielectric sheet. Whispering-gallery modes with radial mode numbers as high as $N = 4$ will fit between the disk edge and the intersection of the pedestal with the disk. Assuming that losses at the outer edge where scattering occurs are minimized while at the same time avoiding losses in the pedestal region where photons will be coupled into the pedestal and substrate region results in an estimate of $N = 3$ for the lasing mode. This model predicts that the surface emission should emanate from the two points of the rhombus shaped pedestal most distant from the center. Some of the lasers did display this mode pattern when imaged on an infrared camera. The polarization was measured to be parallel to the disk radius as expected for the whispering-gallery modes.

Disk geometries have the advantages of smaller total volume and reduced crystal growth time when compared with vertical-cavity surface-emitting laser geometries⁶ with Bragg reflectors where 40 or more quarter-wave layers are often required. The number of layers can, of course, be reduced with high index contrast schemes.⁷ Another important advantage of the disks is the strong optical confinement to the gain region leading to gain enhancements of about twenty over vertical-cavity and horizontal-cavity stripe laser geometries.⁸ The disk modal volume is small enough that essentially only a single mode overlaps the quantum well emission, both spatially and spectrally.

In summary, we have described a new microcavity based on whispering-gallery modes in a thin semiconductor disk. This highly confined optical structure nearly optimizes the overlap of a small volume quantum well gain region with high reflectivity optical modes in high index contrast disks. Our initial experiments show that thin, high index contrast disk structures can be reliably fabricated in the InP/InGaAsP system. These elements may form the basis of efficient microphotonic circuits and arrays.

¹ Lord Rayleigh, "The Problem of the Whispering Gallery," in *Scientific Papers* (Cambridge University, Cambridge, England, 1912), Vol. 5, pp. 617–620.

² C. G. B. Garrett, W. Kaiser, and W. L. Bond, *Phys. Rev.* **124**, 1807 (1961).

³ R. E. Benner, P. W. Barber, F. J. Owen, and R. K. Chang, *Phys. Rev. Lett.* **44**, 475 (1980).

⁴ T. Krauss, P. J. R. Laybourn, and J. Roberts, *Electron. Lett.* **26**, 2097 (1990).

⁵ S. T. Ho, R. E. Slusher, and S. L. McCall, *Quant. Electron. Laser Sci. Tech. Dig.* **11**, 54 (1991).

⁶ J. L. Jewell, Y. H. Lee, S. L. McCall, A. C. Gossard, and J. H. English, *Appl. Phys. Lett.* **53**, 640 (1988).

⁷ S. T. Ho, S. L. McCall, R. E. Slusher, L. N. Pfeiffer, K. W. West, A. F. J. Levi, G. E. Blonder, and J. L. Jewell, *Appl. Phys. Lett.* **57**, 1387 (1990).

⁸ G. P. Agrawal and N. K. Dutta, *Long-Wavelength Semiconductor Lasers* (Reinhold, New York, 1986).